Journal of Zhejiang University-SCIENCE C (Computers & Electronics)
ISSN 1869-1951 (Print); ISSN 1869-196X (Online)
www.zju.edu.cn/jzus; www.springerlink.com
E-mail: jzujedu.cn

# A gain-flatness optimization solution for feedback technology of wideband low noise amplifiers*

Zhen-hua LI, Bang-hong GUO, Zheng-jun WEI[†‡], Song-hao LIU, Nan CHENG, Jin-dong WANG, Jian-jun GUO, Long YAN

(*Key Laboratory of Photonic Information Technology of Guangdong Higher Education Institutes, SIPSE & LQIT, South China Normal University, Guangzhou 510006, China*)

[†]E-mail: weizjweizj@126.com

Received June 28, 2010; Revision accepted Nov. 5, 2010; Crosschecked May 31, 2011

**Abstract:** The ***S*** parameter expression of high-frequency models of the high electron mobility transistors (HEMTs) with basic feedback structure, especially the transmission gain $S_{21}$, is presented and analyzed. In addition, an improved feedback structure and its theory are proposed and demonstrated, in order to obtain a better gain-flatness through the mutual interaction between the series inductor and the parallel capacitor in the feedback loop. The optimization solution for the feedback amplifier can eliminate the negative impacts on transmission gain $S_{21}$ caused by things such as resonance peaks. Furthermore, our theory covers the shortage of conventional feedback amplifiers, to some extent. A wideband low-noise amplifier (LNA) with the improved feedback technology is designed based on HEMT. The transmission gain is about 20 dB with the gain variation of 1.2 dB from 100 MHz to 6 GHz. The noise figure is lower than 2.8 dB in the whole band and the amplifier is unconditionally stable.

**Key words:** Low-noise amplifier (LNA), Ultra-wideband, HEMT, Feedback, Gain flatness
**doi:**10.1631/jzus.C1010300 **Document code:** A **CLC number:** TN722.3

## 1 Introduction

Wideband and ultra-wideband (UWB) low noise amplifiers have attracted extensive research interest over recent years. A wide range of modern and future communication systems that operate over a bandwidth exceeding several gigahertz, such as software-defined radio and UWB, have been proposed. UWB systems are capable of data-transfer rates of up to gigabits per second (Win and Scholtz, 1998; Roy *et al.*, 2004). This poses a more stringent requirement on the UWB transceiver (Scholtz *et al.*, 2000), especially for the front-end low-noise amplifier (LNA), which has to provide an ultra-wide bandwidth with a reasonable noise figure (NF).

The feedback amplifier is one of the most commonly used radio frequency/mm-wave wideband amplifiers. It demonstrates a number of virtues, including good input and output matching, excellent bandwidth, low cost, and easy integration, making it a reliable wideband topology (Gharpurey, 2004; Ismail and Abidi, 2004; Lee and Cressler, 2005; Park *et al.*, 2005; Bahl and Bhartia, 2006). Gain flatness is the key problem of wideband LNA. A classical approach to widening bandwidth is negative feedback, which is normally achieved in the form of resistive shunt feedback (Barras *et al.*, 2004; Kim *et al.*, 2005; Zhan and Taylor, 2006). The resistive feedback allows for good input and output matching from low frequency to high frequency, but it can hardly achieve sufficient bandwidth (Li and Zhang, 2007); the reactive feedback structure obtained with a series inductor $L_f$ added to the resistive feedback loop is often adopted in these feedback-based designs. It can compensate for the inherent decrease of HEMT's gain in high

---

[‡] Corresponding author
[*] Project supported by the Guangdong Key Technologies R & D Program (No. 2007B010400009) and the Guangzhou Science and Technology Pillar Program (No. 2008Z1-D501), China

frequency and counteract the decrease of gain induced by the resistive feedback (Xie *et al.*, 2009). But in this structure of feedback LNA, resonance peaks of transmission gain $S_{21}$ are caused by series inductor $L_f$, transistor's parasitic parameters, and the inductive effect in the feedback loop, and will seriously influence bandwidth and gain flatness of the amplifier. Another reactive feedback structure of the resistive feedback loop with a parallel capacitor $C_f$ added is the ability to also broaden the bandwidth, but with a deterioration of the magnitude of transmission gain of LNA.

In this paper, an improved feedback structure and its theory are proposed and demonstrated, in order to produce a better gain flatness through the mutual interaction between the series inductor and the parallel capacitor in the feedback loop. It could solve the problems associated with the resonance peak and gain deterioration in the reactive feedback structures or resistive feedback structures. In addition, the expression of HEMT's ***S***-parameter with the feedback structure is obtained by analyzing its high-frequency small-signal equivalent model. Different structures of feedback circuit have different influences on the ***S***-parameter, especially on the transmission gain $S_{21}$. To verify our proposed method, a wideband LNA with improved feedback technologies is presented. It is found that theoretical analysis and actual simulation experiments by Agilent ADS agree well. Our theory could remedy the shortage of conventional feedback amplifiers to some extent and further promote the performance of wideband feedback LNA.

## 2 High-frequency model and calculation of negative feedback

Fig. 1a shows a small signal equivalent circuit of the basic HEMT feedback amplifier (Gonzalez, 2006). As is known, at low frequencies, the ***S***-parameters of the feedback amplifier have little dependence on the frequency. But at high frequencies, the parasitic parameters of HEMT should not be ignored. Specifically, both the gate-source junction capacitance $C_{gs}$ and the output conductance $g_{ds}$ greatly influence the properties of the amplifier in the microwave band. With the impacts of $C_{gs}$ and $g_{ds}$ considered and the parasitic parameters of HEMT ignored, the unidirectional high-frequency equivalent modeling of the feedback amplifier will be obtained, as shown in Fig. 1b (Gonzalez, 2006). Thus, we can more accurately analyze the performance of negative feedback amplifier. $L_D$ is a compensating inductor that is often used to compensate the transmission gain at high frequencies for extending the bandwidth and improving the output voltage standing wave ratio (VSWR) (Fu *et al.*, 2010).

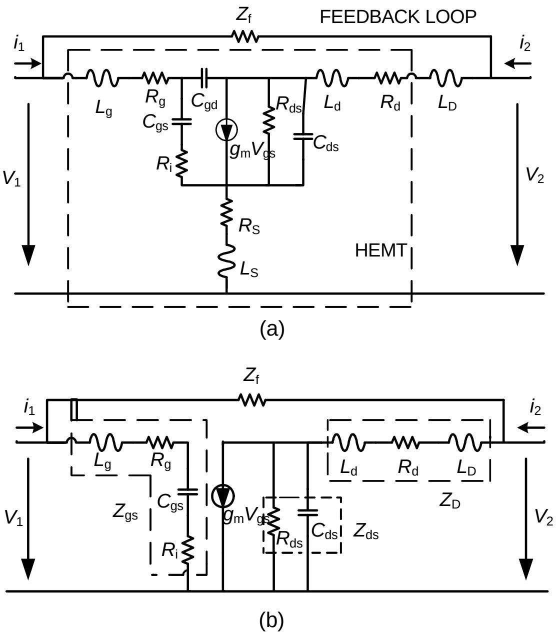


**Fig. 1 Small signal equivalent circuit of the basic HEMT feedback amplifier (a) and unidirectional high-frequency equivalent circuit of HEMT with feedback structure ($C_{gs}$>>$C_{gd}$) (b)**

Based on the above conditions, voltages and currents in Fig. 1b are described by the following Eqs. (1) and (2):

$$i_1 = \frac{Z_f - Z_{gs}}{Z_{gs} Z_f} \cdot V_1 + \frac{1}{Z_f} \cdot V_2, \tag{1}$$

$$\begin{aligned} i_2 = &-\frac{j\omega C_{gs}(Z_D - Z_{ds}) + g_m Z_{gs} Z_{ds} Z_f}{j\omega C_{gs} Z_f (Z_D + Z_{ds})} \cdot V_1 \\ &+ \frac{Z_f + Z_D - Z_{ds}}{Z_f (Z_D + Z_{ds})} \cdot V_2, \end{aligned} \tag{2}$$

where

$$\begin{cases} Z_D = R_d + j\omega L_d + j\omega L_D, \\ Z_{ds} = R_{ds} / (j\omega C_{ds} R_{ds} + 1), \\ Z_{gs} = R_i + R_g + j\omega L_g + 1/(j\omega C_{gs}). \end{cases} \tag{3}$$

Therefore, $Y$-parameters of the equivalent circuit in Fig. 1b are as follows:

$$\begin{pmatrix} \dfrac{Z_\mathrm{f}+Z_\mathrm{gs}}{Z_\mathrm{gs}Z_\mathrm{f}} & -\dfrac{1}{Z_\mathrm{f}} \\ -\dfrac{\mathrm{j}\omega C_\mathrm{gs}(L_\mathrm{D}-Z_\mathrm{ds})+g_\mathrm{m}Z_\mathrm{gs}Z_\mathrm{ds}Z_\mathrm{f}}{\mathrm{j}\omega C_\mathrm{gs}Z_\mathrm{f}(L_\mathrm{D}+Z_\mathrm{ds})} & \dfrac{Z_\mathrm{f}+L_\mathrm{D}-Z_\mathrm{ds}}{Z_\mathrm{f}(L_\mathrm{D}+Z_\mathrm{ds})} \end{pmatrix}. \quad (4)$$

The $\boldsymbol{S}$ parameter of HEMT with feedback is derived from Eq. (4) and represented as

$$\boldsymbol{S}=\begin{pmatrix} S_{11} & S_{12} \\ S_{21} & S_{22} \end{pmatrix}. \quad (5)$$

Its elements are

$$S_{11}=\frac{1}{\varDelta}\left(1-\frac{Z_\mathrm{f}-Z_\mathrm{gs}}{Z_\mathrm{gs}Z_\mathrm{f}}\cdot Z_0\right)\left(1+\frac{Z_\mathrm{f}+L_\mathrm{D}-Z_\mathrm{ds}}{Z_\mathrm{f}(L_\mathrm{D}+Z_\mathrm{ds})}\cdot Z_0\right) -\frac{Z_0^2}{\varDelta\cdot Z_\mathrm{f}}\cdot\frac{\mathrm{j}\omega C_\mathrm{gs}(L_\mathrm{D}-Z_\mathrm{ds})+g_\mathrm{m}Z_\mathrm{gs}Z_\mathrm{ds}Z_\mathrm{f}}{\mathrm{j}\omega C_\mathrm{gs}Z_\mathrm{f}(L_\mathrm{D}+Z_\mathrm{ds})}, \quad (6)$$

$$S_{22}=\frac{1}{\varDelta}\left(1+\frac{Z_\mathrm{f}-Z_\mathrm{gs}}{Z_\mathrm{gs}Z_\mathrm{f}}\cdot Z_0\right)\left(1-\frac{Z_\mathrm{f}+L_\mathrm{D}-Z_\mathrm{ds}}{Z_\mathrm{f}(L_\mathrm{D}+Z_\mathrm{ds})}\cdot Z_0\right) -\frac{Z_0^2}{\varDelta\cdot Z_\mathrm{f}}\cdot\frac{\mathrm{j}\omega C_\mathrm{gs}(L_\mathrm{D}-Z_\mathrm{ds})+g_\mathrm{m}Z_\mathrm{gs}Z_\mathrm{ds}Z_\mathrm{f}}{\mathrm{j}\omega C_\mathrm{gs}Z_\mathrm{f}(L_\mathrm{D}+Z_\mathrm{ds})}, \quad (7)$$

with

$$S_{12}=-\frac{2Z_0}{\varDelta\cdot Z_\mathrm{f}}, \quad (8)$$

$$S_{21}=\frac{2Z_0}{\varDelta}\cdot\frac{\mathrm{j}\omega C_\mathrm{gs}(L_\mathrm{D}-Z_\mathrm{ds})+g_\mathrm{m}Z_\mathrm{gs}Z_\mathrm{ds}Z_\mathrm{f}}{\mathrm{j}\omega C_\mathrm{gs}Z_\mathrm{f}(L_\mathrm{D}+Z_\mathrm{ds})}, \quad (9)$$

$$\varDelta=\left(1+\frac{Z_\mathrm{f}-Z_\mathrm{gs}}{Z_\mathrm{gs}Z_\mathrm{f}}\cdot Z_0\right)\left(1+\frac{Z_\mathrm{f}+L_\mathrm{D}-Z_\mathrm{ds}}{Z_\mathrm{f}(L_\mathrm{D}+Z_\mathrm{ds})}\cdot Z_0\right) -\frac{1}{Z_\mathrm{f}}\cdot\frac{\mathrm{j}\omega C_\mathrm{gs}(L_\mathrm{D}-Z_\mathrm{ds})+g_\mathrm{m}Z_\mathrm{gs}Z_\mathrm{ds}Z_\mathrm{f}}{\mathrm{j}\omega C_\mathrm{gs}Z_\mathrm{f}(L_\mathrm{D}+Z_\mathrm{ds})}\cdot Z_0^2. \quad (10)$$

As shown in Eq. (9), trans-conductance $g_\mathrm{m}$, feedback impedances $Z_\mathrm{f}$, $L_\mathrm{D}$, $Z_\mathrm{ds}$, and $Z_\mathrm{gs}$ jointly determine the amplitude of $S_{21}$. But the gain of HEMT decreases at the rate of 6 dB/octave when the frequency increases due to several intrinsic parasitic parameters. Thus, it is necessary to compensate and counterpoise the whole frequency response to the HEMT with reactive elements in the feedback loop. The gain flatness in the UWB can be realized with proper values of feedback impedance $Z_\mathrm{f}$.

## 3 Improved feedback structure and comparison with other feedback structures

The reactive feedback amplifier with an RL feedback network in Fig. 2a contains two series inductors, $L_\mathrm{D}$ in the drain line and $L_\mathrm{f}$ in the feedback loops. Fig. 2b shows another reactive feedback structure with an RC feedback network. According to Eq. (9), transmission gains of the two circuits in Figs. 2a and 2b are calculated and demonstrated in Figs. 3 and 4, respectively. For the further insight into the LNA, the typical value of each parameter used in the calculation is listed in Table 1 (Wang *et al.*, 1992).

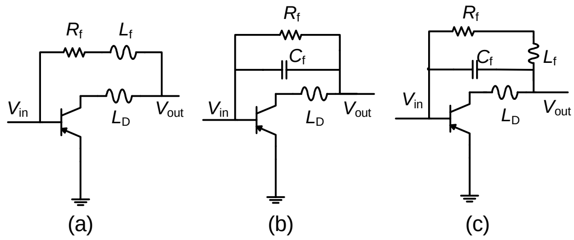


**Fig. 2 Schematic circuit of the basic feedback amplifier**
(a) RL feedback network; (b) RC feedback network; (c) Improved feedback network

**Table 1 Typical parameters used in the calculation**

| Parameter | Value | Parameter | Value |
|---|---|---|---|
| $g_\mathrm{m}$ (S) | 0.20 | $C_\mathrm{ds}$ (fF) | 19 |
| $C_\mathrm{gs}$ (fF) | 27.1 | $L_\mathrm{D}$ (nH) | 0.2 |
| $R_\mathrm{i}$ (Ω) | 1.4 | $R_\mathrm{f}$ (Ω) | 180 |
| $R_\mathrm{ds}$ (Ω) | 531 | $f$ (GHz) | 0–10 |

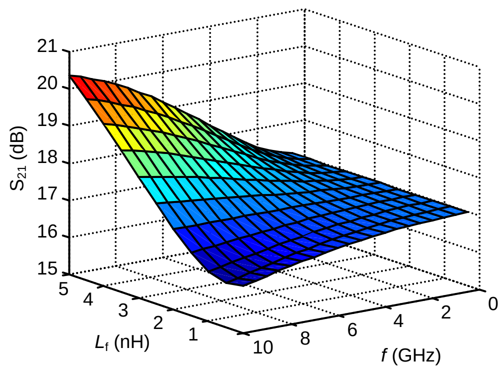


**Fig. 3 Dependence of $S_{21}$ on frequency and $L_\mathrm{f}$ in Fig. 2a when $R_\mathrm{f}$=180 Ω**

By varying the values of the inductor $L_\mathrm{f}$ and capacitor $C_\mathrm{f}$, their influence on insertion gain and bandwidth of the amplifier in Fig. 1 is well demonstrated. This comparison is presented in Figs. 3 and 4 for a series of selected combinations of $L_f$ and $C_f$. The curves clearly demonstrate the influence of $L_f$ and $C_f$ on the bandwidth and gain response of the basic feedback amplifier.

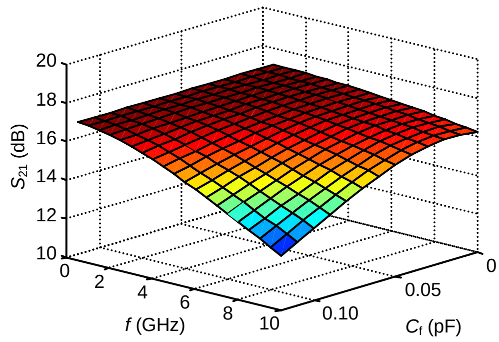


**Fig. 4 Dependence of $S_{21}$ on frequency and $C_f$ in Fig. 2b when $R_f$=180 Ω**

When the series inductor $L_f$ and parallel capacitor $C_f$ are both close to zero, a small value $C_{gs}$ (27.1 fF as given in Table 1) causes a small gain reduction as the frequency increases from 0 to 10 GHz (Figs. 3 and 4).

For the series inductor $L_f$ in Fig. 2a, when the value changes from 0 to 5 nH, the transmission gain $S_{21}$ increases from 16.2 dB to nearly 22.4 dB as the frequency increases from 0 to 10 GHz. For the parallel capacitor $C_f$ in Fig. 2b, when its value changes from 0 to 0.12 pF, the transmission gain $S_{21}$ decreases from about 16.5 to 12.8 dB as the frequency increases from 0 to 10 GHz.

The reactive feedback amplifier with an RL feedback network (Fig. 2a) contains two series inductors in the feedback loops, which have been inserted to extend the bandwidth of the amplifier. However, in practical circuit design, the series inductor $L_f$, transistor's parasitic parameters, and the inductive effect in the feedback loop would induce resonance peaks of the $S_{21}$ curves. Though the two inductors, $L_f$ and $L_D$, could compensate the transmission gains at high frequencies to extend the bandwidth of the amplifier (Xie *et al.*, 2009; Fu *et al.*, 2010), the resonance peaks would cause an evident deterioration of the gain flatness.

The reactive feedback structure with an RC feedback network (Fig. 2b) can also broaden the bandwidth, but it deteriorates the magnitude of the transmission gain of LNA.

Therefore, we present an improved topology which uses a series inductor and a parallel capacitor in the feedback loop simultaneously (Fig. 2c).

To obtain a detailed comparison, we choose a value of $L_f$ arbitrarily, for example, 3.9 nH, and we will find that the parallel capacitor $C_f$ and the series inductor $L_f$ play a role of mutual compensation and balance in the peak of gain (Fig. 5a).

The dependence of $S_{21}$ on both the series inductor $L_f$ and the parallel capacitor $C_f$ is well demonstrated in Fig. 5b, which is the side view of Fig. 5a. It is clear that there is an optimum parallel capacitor value that makes the $S_{21}$ curve flat with 0.2 dB of gain variation in the whole band from 0 to 10 GHz; this value is approximately 0.045 pF.

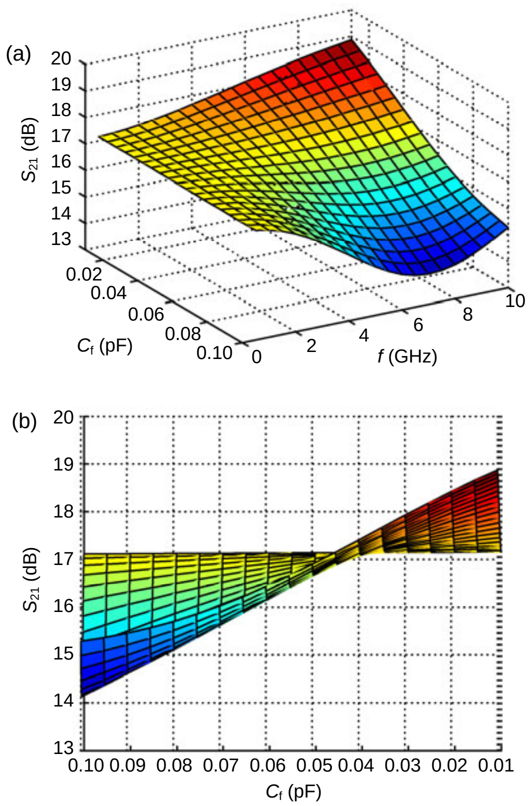


**Fig. 5 Dependence of $S_{21}$ on frequency and $C_f$ in Fig. 2c when $L_f$=3.9 nH, $R_f$=180 Ω**

(b) is the side view of (a)

Reactive elements in the feedback loop can adjust the magnitude and phase of the feedback current $I_f$. The series inductor $L_f$ enhances the amount of feedback at low frequencies, while reducing the amount at high frequencies. In addition, the parallel capacitor $C_f$ can enhance the amount of feedback at low frequencies, while reducing the amount at high frequencies. A reactance component can produce a pole on transmission gain $S_{21}$, so we use two reactance components to control the feedback current $I_f$ at different frequencies. By the superposition of the two reverse poles, the resonance peaks on transmission gain $S_{21}$ could be suppressed and eliminated, which improves flatness compared to conventional feedback amplifiers.

## 4 Validation results and discussion

An amplifier was designed based on the Agilent ATF-551M4 low noise enhancement mode pseudomorphic HEMT (EpHEMT) in two stages. ATF-551M4 was supplied in a leadless surface-mount plastic package with dimensions of 1.4 mm×1.2 mm ×0.7 mm, and its 400-μm gate width combines low noise figure coincident with high intercept point.

Fig. 6 shows the schematic diagram of the wideband LNA. This circuit uses multiple stages with the improved feedback structure to improve the gain and gain flatness. Here, the DC source of 5 V supplies DC bias of two transistors through $R_1$–$R_6$. $C_1$–$C_4$ and $L_1$–$L_4$ are bypass capacitors and choke inductors, respectively. Both $C_5$ and $C_6$ are 0.1 pF. $L_5$ and $L_6$ equal 0.6 nH. Both of the input and output networks are composed of resistances and microstrip lines.

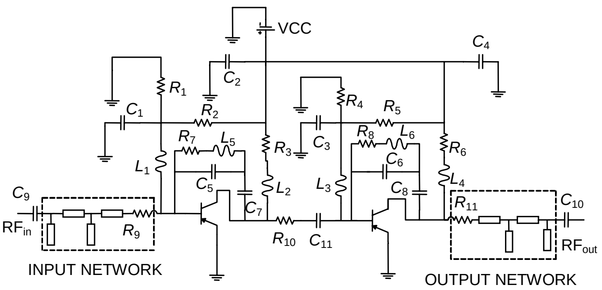


**Fig. 6 Schematic circuit of the wideband LNA**

The schematic circuit was simulated with Agilent ADS. As a three-dimensional electromagnetic simulator of ADS, Momentum is able to generate accurate EM models during simulation. We used co-simulation with schematic and momentum based on methods of moments. Actual models of capacitor and inductor in the above circuit were adopted from the Murata Components Library for Agilent ADS. The accuracy and efficiency of simulations have been improved, since physical effects of the layout components were taken into account. The transmission gain $S_{21}$ (Fig. 7) is approximately 20 dB with only 1.2 dB of gain variation from 100 MHz to 6 GHz. Fig. 8 shows the other performance parameters of the wideband LNA. The noise figure in the whole band is lower than 2.8 dB, and VSWRs of the input port and output port are both lower than 2.4.

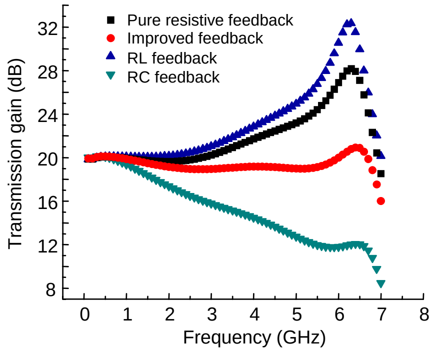


**Fig. 7 Transmission gain $S_{21}$ of the two-stage wideband LNA**

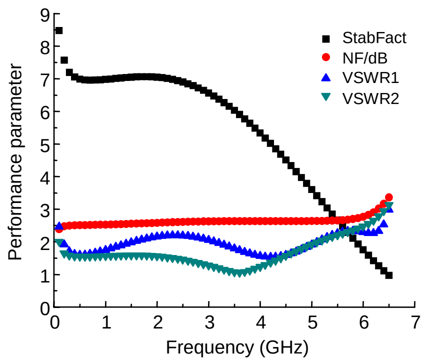


**Fig. 8 Performance of the two-stage wideband LNA**

As a comparison, Fig. 7 also gives the gain curves of LNA adopting the other reactive feedback networks. Evident resonance peak occurs at about 6.3 GHz in the $S_{21}$ curve of LNA with the RL feedback network (without parallel capacitor $C_5$ or $C_6$ in the feedback loop). A similar resonance peak occurs in LNA with the pure resistive negative feedback network. When the RC feedback network (without series inductor $L_5$ or $L_6$) is adopted, the gain declines from 20 to 12 dB. When we adopt the improved feedback network (with both parallel capacitors and series inductors added to the feedback loops), the gain peak can be eliminated, and the gain curve becomes flat with 1.2 dB of gain variation from 100 MHz to 6 GHz.

Although the improved feedback structure is an efficient gain flatness optimization solution, it has some limitations. For example, it may deteriorate the stability of the feedback LNA to some extent. Thus, we can make a compromise between the different performance parameters. We could choose proper feedback structures and component parameters according to our demands in practical circuit design.

## 5 Conclusions

An improved topological structure and its corresponding theory are presented to obtain a better performance of the feedback wideband LNA through the mutual interaction between the series inductor and parallel capacitor in the feedback loop. The optimization solution of the feedback amplifier based on this theory can eliminate resonance peaks on transmission gain $S_{21}$ very well. Furthermore, our theory overcomes several shortcomings of the conventional feedback amplifier. A wideband LNA with the improved feedback technology is designed based on the Agilent ATF-551M4 low noise enhancement mode pseudomorphic HEMT. The transmission gain is about 20 dB with the gain variation of 1.2 dB from 100 MHz to 6 GHz. The noise figure is lower than 2.8 dB in the whole band and the amplifier is unconditionally stable.

## References


Bahl, I., Bhartia, P., 2006. Microwave Solid State Circuit Design (2nd Ed.). Publishing House of Electronics Industry, Beijing, China, p.366-378 (in Chinese).

Barras, D., Ellinger, F., Jackel, H., Hirt, W., 2004. A low supply voltage SiGe LNA for ultra-wideband frontends. *IEEE Microw. Wirel. Compon. Lett.*, **14**(10):469-471. [doi:10.1109/LMWC.2004.834556]

Fu, C.T., Kuo, C.N., Taylor, S.S., 2010. Low noise amplifier design with dual reactive feedback for broadband simultaneous noise and impedance matching. *IEEE Trans. Microw. Theory Techn.*, **58**(4):795-806. [doi:10.1109/TMTT.2010.2041570]

Gharpurey, R., 2004. A Broadband Low-Noise Front-End Amplifier for Ultra Wideband in 0.13-μm CMOS. Proc. IEEE Custom Integrated Circuits Conf., p.605-608. [doi:10.1109/CICC.2004.1358898]

Gonzalez, G., 2006. Microwave Transistor Amplifiers Analysis and Design (2nd Ed.). Publishing House of Tsinghua University, Beijing, China, p.366-378 (in Chinese).

Ismail, A., Abidi, A.A., 2004. A 3-10-GHz low-noise amplifier with wideband LC-ladder matching network. *IEEE J. Sol.-State Circ.*, **39**(12):2269-2277. [doi:10.1109/JSSC.2004.836344]

Kim, C.W., Kang, M.S., Anh, P.T., Kim, H.T., Lee, S.G., 2005. An ultra wideband CMOS low-noise amplifier for 3-5-GHz UWB system. *IEEE J. Sol.-State Circ.*, **40**(2):544-547. [doi:10.1109/JSSC.2004.840951]

Lee, J., Cressler, J.D., 2005. A 3-10 GHz SiGe Resistive Feedback Low Noise Amplifier for UWB Applications. IEEE Radio Frequency Integrated Circuits Symp., p.545-548. [doi:10.1109/RFIC.2005.1489871]

Li, Q., Zhang, Y.P., 2007. A 1.5-V 2–9.6-GHz inductorless low-noise amplifier in 0.13-μm CMOS. *IEEE Trans. Microw. Theory Techn.*, **55**(10):2015-2023. [doi:10.1109/TMTT.2007.905495]

Park, Y., Lee, C.H., Cressler, J.D., Laskar, J., Joseph, A., 2005. A Very Low Power SiGe LNA for UWB Application. IEEE MTT-S Int. Microwave Symp., p.1041-1044. [doi:10.1109/MWSYM.2005.1516847]

Roy, S., Foerster, J.R., Somayazulu, V.S., Leeper, D.G., 2004. Ultrawideband radio design: the promise of high-speed, short-range wireless connectivity. *Proc. IEEE*, **92**(2):295-311. [doi:10.1109/JPROC.2003.821910]

Scholtz, R.A., Weaver, R., Homier, E., Lee, J., Hilmes, P., Taha, A., Wilson, R., 2000. UWB Radio Deployment Challenges. 11th IEEE Int. Symp. on Personal, Indoor and Mobile Radio Communications, p.620-625. [doi:10.1109/PIMRC.2000.881497]

Wang, H., Dow, G.S., Allen, B.R., Ton, T.N., Tan, K.L., Chang, K.W., Chen, T.H., Berenz, J., Lin, T.S., Liu, P.H., *et al.*, 1992. High-performance in W-band monolithic pseudomorphic InGaAs HEMT LNA's and design/analysis methodology. *IEEE Trans. Microw. Theory Techn.*, **40**(3):417-428. [doi:10.1109/22.121716]

Win, M.Z., Scholtz, R.A., 1998. Impulse radio: how it works. *IEEE Commun. Lett.*, **2**(2):36-38. [doi:10.1109/4234.660796]

Xie, H.Y., Zhang, W.R., Li, J., Shen, P., Huang, Y.W., Huang, L., Hu, N., 2009. Study of Feedback Technology for Gain Flatness of UWB LNA. 3rd IEEE Int. Symp. on Microwave Antenna, Propagation and EMC Technologies for Wireless Communications, p.466-469. [doi:10.1109/MAPE.2009.5355634]

Zhan, J.H.C., Taylor, S.S., 2006. A 5GHz Resistive-Feedback CMOS LNA for Low-Cost Multi-standard Applications. IEEE Int. Solid-State Circuits Conf., p.721-730. [doi:10.1109/ISSCC.2006.1696111]